

Efficient Q-RTM in transversely isotropic media

Wenyi Hu*, Advanced Geophysical Technology Inc., Tong Zhou, and Jieyuan Ning, Peking University

Summary

In order to compensate the Q effect in anisotropic visco-acoustic media, we developed an efficient finite-difference Q-RTM algorithm applicable to both vertical transversely isotropic (VTI) and tilted transversely isotropic (TTI) scenarios. This anisotropic Q-RTM algorithm is able to substantially improve the earth imaging quality below visco-acoustic overburdens, such as gas cloud and gas chimney, in complicated geological settings.

The main bottleneck of most existing Q-RTM algorithms is the high computational expense due to the pseudo-spectral operators employed by these methods for the evaluation of fractional derivatives. To mitigate this difficulty, we developed a so-called multi-stage optimized negative τ method as the propagation engine for Q compensation. The unique feature of this propagation engine that distinguishes it from other methods is that it is based on the finite-difference method instead of the pseudo-spectral method. This feature saves the computational expense significantly and simplifies the code parallelization and GPU implementation, especially for large scale projects. This finite-difference based propagation engine with Q compensation capability consists of two main components: 1) the negative τ scheme that accurately boosts the amplitude of the attenuated seismic data during the migration procedure without affecting the system stability; 2) the multi-stage dispersion optimization scheme that precisely recovers the phase distortion in the attenuated seismic data and correct the phase velocity deviation caused by the negative τ scheme.

Both the theoretical analysis and the numerical experiments validated the computational efficiency of this anisotropic Q-RTM method, which is comparable to a regular finite-difference RTM without Q compensation. The numerical example shows that the missing or blurred structural features in the regular RTM image below Q zones are accurately reconstructed.

Introduction

Seismic wave loses energy when propagates through attenuating media, such as fluid-saturated reservoirs and gas clouds, causing two main effects: the amplitude reduction and the phase change. These two main effects have negative impacts on images if these attenuated seismic data are migrated using conventional RTM methods, observed as dimming structures below the visco-acoustic overburdens, spatial resolution reduction, geological structure depth shift, wavelet shape distortion, structural

detail loss, etc. To enhance the earth imaging quality, various Q compensation technologies have been developed, including the inverse Q filtering (Bickel and Natarajan, 1985; Hargreaves, 1991), the Kirchhoff Q-migration (Traynin et al., 2008), Q-WEM (Dai and West, 1994; Yu et al., 2002), and Q-RTM. Because Q-RTM (Zhang et al., 2010; Zhu et al., 2014; Hu et al., 2016) includes the full physics, it is believed to be the most accurate and powerful tool of Q-compensated imaging, especially for complicated geological settings where anisotropic properties have to be taken into account.

Most of the existing Q-RTM algorithms are based on the pseudo-spectral method (Zhang et al., 2010; Zhu et al., 2014), in which global operators (i.e., FFT and inverse FFT) are employed to evaluate the fractional derivatives in the governing equations of Q-compensated wave propagation. Suh et al. (2012) extended the pseudo-spectral based Q-RTM to accommodate VTI medium. The main concern of this category of Q-RTM methods is the computational efficiency issue associated with the global nature of FFT operators. For large industrial sized 3D projects, domain decomposition might be necessary for the purpose of parallelization and GPU implementation, which increases the complexity level dramatically and can even be prohibitive. Due to this fact, a local differential operator based Q-RTM approach is more preferable. Unfortunately, simple extension of the widely used finite-difference based Q attenuation propagator (Blanch et al., 1995) to Q-compensated propagation does not properly correct the phase distortion brought by the Q effects (Guo et al., 2016) although the amplitudes can be boosted successfully.

In this work, we developed an anisotropic Q-RTM method based on finite-difference operators. This anisotropic Q-RTM method, applicable to both VTI and TTI cases, is the generalization of our previously reported isotropic Q-RTM algorithm (Hu et al., 2016). To employ finite-difference operators for Q-compensated wave propagation without ruining the system stability, we propose a negative τ method. In the negative τ method, auxiliary memory variables are introduced to accurately compensate the amplitude reduction by approximating the fractional derivative using the finite-difference operator. Unfortunately, the negative τ scheme alone is not sufficient to solve the problem. Although the decayed amplitudes are brought back successfully by the negative τ method, the incorrect phase in the attenuated seismic data is further distorted by the extra terms of auxiliary memory variables. To correct this frequency-dependent phase change, we modify the governing equations by adding multiple dispersion optimization terms to match the ideal dispersion

Finite-Difference Q-RTM for TI media

relation curves in all propagation directions. These dispersion optimization terms are specially designed to be numerically evaluated by finite-difference operators. We need to mention that Q is assumed to be isotropic in this work but the seismic velocity is anisotropic.

Stabilized Pseudo-acoustic TTI Wave Equation

Without considering the Q compensation, the pseudo-acoustic TTI wave equation can be derived by solving the Christoffel equations (Tsvankin, 2001) by setting the phase velocity of SV mode to zero (Fletcher et al., 2009):

$$\begin{aligned} \frac{\partial^2 p}{\partial t^2} &= v_{px}^2 H_2 p + a v_{pz}^2 H_1 q + v_{sz}^2 H_1 (p - a q) \\ \frac{\partial^2 q}{\partial t^2} &= \frac{v_{pm}^2}{a} H_2 p + v_{pz}^2 H_1 q + v_{sz}^2 H_2 \left(\frac{1}{a} p - q \right) \end{aligned} \quad (1)$$

where p is the pressure wavefield and q is the auxiliary wavefield, v_{pz} is the P -wave velocity in the direction normal to the symmetry plane, $v_{px} = v_{pz} \sqrt{1 + 2\varepsilon}$ is the P -wave velocity in the symmetry plane, $v_{pm} = v_{pz} \sqrt{1 + 2\delta}$ is the P -wave NMO velocity normal to the symmetry plane, v_{sz} is the SV velocity normal to the symmetry plane, ε and δ are the anisotropic parameters with weak anisotropic approximation (Thomsen, 1986), and the nonzero parameter a is set to 1 in our implementation. The differential operators H_1 and H_2 for two-dimensional cases are defined as

$$\begin{aligned} H_1 &= \sin^2 \theta \frac{\partial^2}{\partial x^2} + \sin 2\theta \frac{\partial^2}{\partial x \partial z} + \cos^2 \theta \frac{\partial^2}{\partial z^2} \\ H_2 &= \cos^2 \theta \frac{\partial^2}{\partial x^2} - \sin 2\theta \frac{\partial^2}{\partial x \partial z} + \sin^2 \theta \frac{\partial^2}{\partial z^2} \end{aligned} \quad (2)$$

where θ is the dip angle to the vertical direction.

Negative τ Method for Amplitude Compensation

Mathematically, without modifying the original wave equation form, the Q attenuation effect can be easily incorporated into the wave equations by generalizing the real wave velocity to a complex wave velocity. In other words, the imaginary part of the complex wave velocity describes the attenuation behavior of a wave propagating through a lossy medium. With this observation, Blanch et al. (1995) reported an efficient method, the τ method, to approximate a constant Q (i.e., frequency independent Q) for viscoelastic wave propagation simulations. The most important advantage of the τ method is that, with the introduction of memory variables and the corresponding auxiliary equations, the fractional derivative evaluation and the convolution operations are avoided. This advantage makes the local operator based numerical method, such as finite-difference method, can be directly employed for

wave propagation simulation within lossy media. In the τ method, the complex phase velocity is designed to be

$$v_p^A(\omega) = v_0 \sqrt{1 + \sum_{l=1}^L \frac{i\omega\tau_l}{1 + i\omega\tau_l}}, \quad (3)$$

where the superscript A denotes a Q attenuation process. In formulation (3), the constant Q effect over a predefined frequency range is approximated by the polynomials, where L is the number of relaxation mechanisms. Usually 3 to 5 relaxation mechanisms with the optimized parameters τ and τ_σ (both are positive real numbers) are accurate enough to achieve a relatively constant Q over the frequency range of migration.

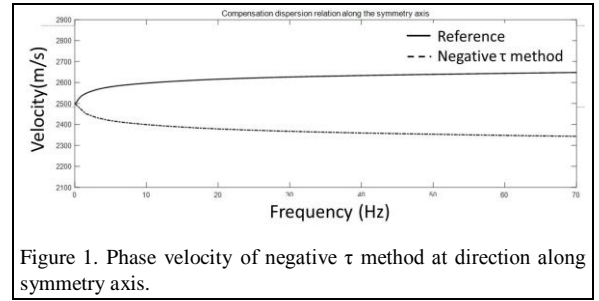


Figure 1. Phase velocity of negative τ method at direction along symmetry axis.

In Q-RTM, the Q attenuation effect needs to be replaced by the Q compensation for both the source-side and receiver-side propagation. This can be realized by changing the sign of the imaginary part of the complex phase velocity without changing the real part. Flipping the sign of the imaginary part is equivalent to replacing the positive Q values by the negative Q. Keeping the real part of the complex phase velocity unchanged is critical because the dispersion relation of the Q-compensated propagation in a Q-RTM process must remain the same as that of the Q-attenuated propagation process in order to migrate the seismic energy to the correct locations in the subsurface. In other words, the complex phase velocity of a Q-compensated propagator must be the conjugate of the phase velocity of Q-attenuation, i.e., $v_p^A = \overline{v_p^C}$, where $\overline{*}$ represents conjugate and the superscript C denotes Q compensation. Observing (3), an ideal scheme is to negate τ_σ , which results in a perfect negative Q and a perfect phase velocity. Unfortunately, this scheme is impractical because a negative τ_σ causes an unconditionally unstable system.

For this reason, we propose an alternative approach, the negative τ method. Instead of changing the sign of τ_σ , we negate τ . The negative τ method yield the same imaginary part of the phase velocity as the negative τ_σ scheme, implying the amplitude will be properly boosted during the wave propagation. However, the real part of the phase velocity is different from formulation (3). As shown in Figure 1, the phase velocity deviates from the proper

Finite-Difference Q-RTM for TI media

velocity severely and this deviation increases with frequency. Consequently, not only the seismic energy cannot be migrated to the correct positions in the subsurface but also the shapes of the wavelets will be further distorted, increasing the ambiguity and uncertainty in geological interpretation.

Multi-Stage Dispersion Optimization

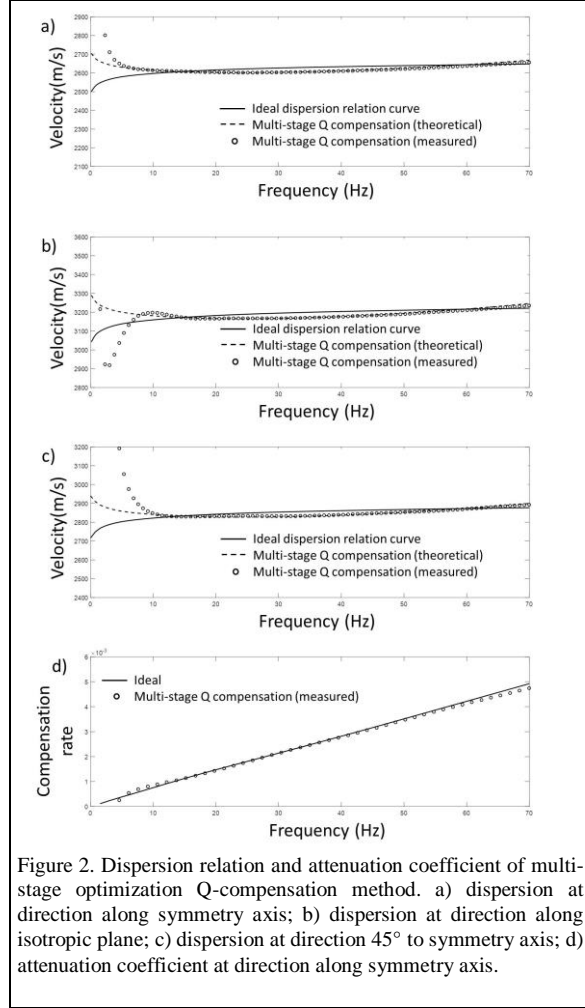


Figure 2. Dispersion relation and attenuation coefficient of multi-stage optimization Q-compensation method. a) dispersion at direction along symmetry axis; b) dispersion at direction along isotropic plane; c) dispersion at direction 45° to symmetry axis; d) attenuation coefficient at direction along symmetry axis.

To mitigate the phase velocity deviation problem, we developed a multi-stage dispersion optimization method to modify the phase velocity of the negative τ method to

$$v_p^C(\omega) = v_0 \sqrt{1 - \sum_{l=1}^L \frac{i\omega\tau_l\tau_{ol}}{1 + i\omega\tau_{ol}}} + M(\omega), \quad (4)$$

where $M(\omega)$ is the multi-stage dispersion optimization term $M(\omega) = \alpha + \beta\omega^2 + \gamma\omega^4$. (5)

Here, α , β , and γ are called 1st-, 2nd-, and 3rd-stage optimization parameters, introduced to adjust the dispersion relation curve of the negative τ method over a certain frequency range. These dispersion optimization parameters are obtained by solving the following inverse problem

$$\min \left\| v_p^C(\omega, \alpha, \beta, \gamma) - v_p^A(\omega) \right\|^2. \quad (6)$$

The 1st-stage optimization term, which is frequency independent, shifts the dispersion curve upward or downward to approximately correct the average phase velocity over the frequency range of interest. The 2nd-stage optimization term modify the curvature of the dispersion curve to match the reference curve v_p^A while the 3rd-stage optimization term fine tunes the shape of the curve to further reduce the mismatch. A very important feature of the multi-stage optimization method is that the parameters α , β , and γ are independent of velocity. Instead, they are determined by the Q value and the frequency range of interest. With this observation, one is able to set up a general optimization parameter lookup table outside of the Q-RTM engine to save the recalculation cost.

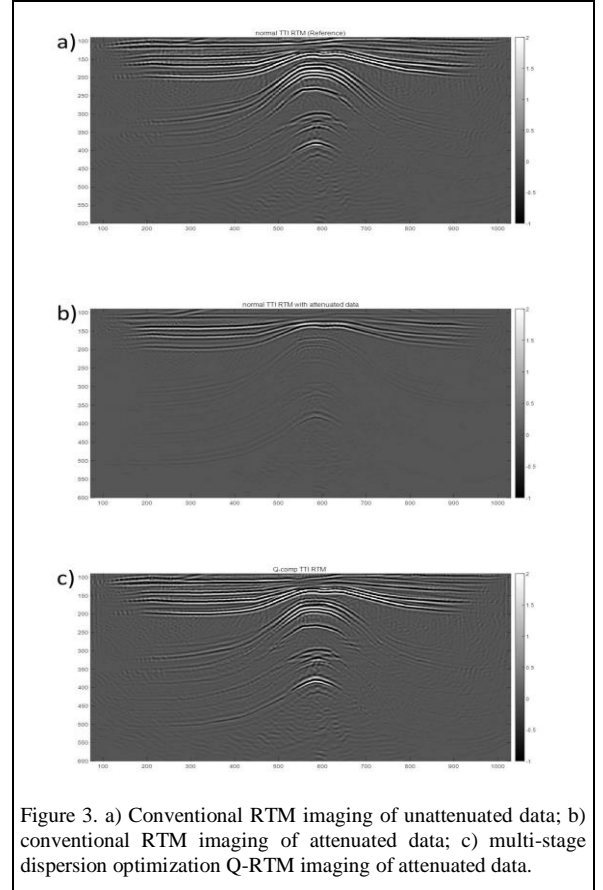


Figure 3. a) Conventional RTM imaging of unattenuated data; b) conventional RTM imaging of attenuated data; c) multi-stage dispersion optimization Q-RTM imaging of attenuated data.

Finite-Difference Q-RTM for TI media

Another advantage of this method is that the dispersion optimization scheme (4) remains the same for different propagation directions as long as Q is isotropic. Because of this advantage, in practice, formulation (4) can easily be extended to a TTI case by modifying the governing equation (1) to

$$\begin{aligned} \omega^2 p &= \left(v_{px}^2 \hat{k}_x^2 p + a v_{pz}^2 \hat{k}_z^2 q \right) \left(1 - \sum_{l=1}^L \frac{i \omega \tau \tau_{cl}}{1 + i \omega \tau_{cl}} + M(\omega) \right) \\ &+ v_{sz}^2 \hat{k}_z^2 (p - a q) \\ \omega^2 q &= \left(\frac{1}{a} v_{pn}^2 \hat{k}_x^2 p + v_{pz}^2 \hat{k}_z^2 q \right) \left(1 - \sum_{l=1}^L \frac{i \omega \tau \tau_{cl}}{1 + i \omega \tau_{cl}} + M(\omega) \right), \\ &+ v_{sz}^2 \hat{k}_z^2 \left(\frac{1}{a} p - q \right) \end{aligned} \quad (7)$$

where \hat{k} is the wavenumber under local coordinates. If Q is anisotropic, then an extra set of dispersion optimization parameters need to be added in the governing equation but the procedure is similar and straightforward.

For ease of implementation, equation (7) can be written in the following form by introducing the memory variables u , v , and the correction variables p^O , q^O :

$$\begin{aligned} \frac{\partial^2 p}{\partial t^2} &= (1 + L \tau) \left[v_{px}^2 H_2 (p + p^O) + a v_{pz}^2 H_1 (q + q^O) \right] \\ &- \sum_{l=1}^L u_l + v_{sz}^2 H_1 (p - a q) \\ \frac{\partial^2 q}{\partial t^2} &= (1 + L \tau) \left[\frac{v_{pn}^2}{a} H_2 (p + p^O) + v_{pz}^2 H_1 (q + q^O) \right] \\ &- \sum_{l=1}^L v_l + v_{sz}^2 H_2 \left(\frac{1}{a} p - q \right) \end{aligned} \quad (8)$$

where

$$\begin{aligned} \frac{\partial u_l}{\partial t} &= \frac{\tau}{\tau_{cl}} \left(v_{px}^2 H_2 p + a v_{pz}^2 H_1 q \right) - \frac{1}{\tau_{cl}} u_l \\ \frac{\partial v_l}{\partial t} &= \frac{\tau}{\tau_{cl}} \left(\frac{1}{a} v_{pn}^2 H_2 p + v_{pz}^2 H_1 q \right) - \frac{1}{\tau_{cl}} v_l \end{aligned} \quad (9)$$

and the correction variables can be approximated by

$$\begin{aligned} p^O &\approx \alpha p - \beta \left[v_{px}^2 H_2 p + a v_{pz}^2 H_1 q + v_{sz}^2 H_1 (p - a q) \right] \\ q^O &\approx \alpha q - \beta \left[\left(\frac{v_{pn}^2}{a} H_2 p + v_{pz}^2 H_1 q \right) + v_{sz}^2 H_2 \left(\frac{p}{a} - q \right) \right] \end{aligned} \quad (10)$$

The 3rd-stage optimization term in (10) is omitted because the two-stage optimization is usually sufficient for most TTI Q-RTM applications. More stages of optimization theoretically improve the accuracy but increase the computation expense and may affect the system stability.

Figure 2 shows the phase velocity of the multi-stage optimization Q-compensation method along the symmetry axis, the isotropic plane, and 45° to the symmetry axis, respectively. Apparently, the dispersion relation curve mismatch shown in Figure 1 is reduced significantly. The numerically measured phase velocity is also shown in the figure, which is consistent to the analytical dispersion analysis. Figure 2d) is the compensation rate defined as

$$R(\omega) = \frac{\omega}{v_p(\omega)Q}. \quad (11)$$

This parameter quantitatively defines the amplitude boost rate as a function of frequency. With the multi-stage optimization method, the numerically measured compensation rate and the analytical compensation rate are in good agreement. As a conclusion, equation (8) to (10) simultaneously compensate the amplitude and the phase distortion. Because there is no fractional derivative in these equations, finite-difference method can be directly used as the Q-RTM engine.

Numerical Implementation and Example

We construct a TTI velocity model by truncating the BP2007 model. First, a set of synthetic data was generated without any attenuation and the dataset is input into a conventional RTM algorithm to produce the image shown in Figure 3a). Then, a laterally extended Q zone is added in the shallow region and another set of synthetic data was generated with the attenuation effect. With this dataset, the conventional RTM is unable to clearly image the structures below the Q zone, as shown in Figure 3b). Resolution loss and wavelet distortion are observed. With the same dataset, the TTI Q-RTM was performed and the imaging result is shown in Figure 3c), which is almost identical to Figure 3a). This numerical experiment demonstrated the effectiveness of this new TTI Q-RTM algorithm.

Conclusions and Discussions

We successfully developed an efficient Q-RTM algorithm for TI medium to enhance the imaging quality in complicated geological settings where visco-acoustic overburden is in presence. Because of the two unique techniques we developed, the negative τ method and the multi-stage dispersion optimization approach, this algorithm is able to avoid the fractional derivative evaluation in a Q-compensated propagation process, saving the computational expense significantly. For the first time, amplitude and phase are compensated simultaneously with high accuracy within the RTM engine based a finite-difference method in TTI media. The numerical experiment validated the accuracy and the efficiency of this new TTI Q-RTM algorithm.

Finite-Difference Q-RTM for TI media

References

- Bickel, S.H. and Natarajan, R.R., 1985. Plane-wave Q deconvolution. *Geophysics*, 50(9), pp.1426-1439.
- Blanch, J.O., Robertsson, J.O. and Symes, W.W., 1995. Modeling of a constant Q: Methodology and algorithm for an efficient and optimally inexpensive viscoelastic technique. *Geophysics*, 60(1), pp.176-184.
- Dai, N. and West, G.F., 1994, January. Inverse Q migration. In 1994 SEG Annual Meeting. Society of Exploration Geophysicists.
- Fletcher, R.P., Du, X. and Fowler, P.J., 2009. Reverse time migration in tilted transversely isotropic (TTI) media. *Geophysics*, 74(6), pp.WCA179-WCA187.
- Guo, P., McMechan, G.A. and Guan, H., 2016. Comparison of two viscoacoustic propagators for Q-compensated reverse time migration. *Geophysics*, 81(5), pp.S281-S297.
- Hargreaves, N.D. and Calvert, A.J., 1991. Inverse Q filtering by Fourier transform. *Geophysics*, 56(4), pp.519-527.
- Hu, W., Zhou, T. and Ning, J., 2016. An efficient Q-RTM algorithm based on local differentiation operators. In SEG Technical Program Expanded Abstracts 2016 (pp. 4183-4187). Society of Exploration Geophysicists.
- Suh, S., Yoon, K., Cai, J. and Wang, B., 2012, November. Compensating visco-acoustic effects in anisotropic reverse-time migration. In 2012 SEG Annual Meeting. Society of Exploration Geophysicists.
- Thomsen, L., 1986. Weak elastic anisotropy. *Geophysics*, 51(10), pp.1954-1966.
- Traynin, P., Liu, J. and Reilly, J.M., 2008, January. Amplitude and bandwidth recovery beneath gas zones using Kirchhoff prestack depth Q-migration. In 2008 SEG Annual Meeting. Society of Exploration Geophysicists.
- Tsvankin, I., 2012. Seismic signatures and analysis of reflection data in anisotropic media. Society of Exploration Geophysicists.
- Yu, Y., Lu, R.S. and Deal, M.M., 2002, January. Compensation for the effects of shallow gas attenuation with viscoacoustic wave-equation migration. In SEG Technical Program Expanded Abstracts (Vol. 21, pp. 2062-2065).
- Zhang, Y., Zhang, P. and Zhang, H., 2010, January. Compensating for visco-acoustic effects in reverse-time migration. In 2010 SEG Annual Meeting. Society of Exploration Geophysicists.
- Zhu, T., Harris, J.M. and Biondi, B., 2014. Q-compensated reverse-time migration. *Geophysics*, 79(3), pp.S77-S87.